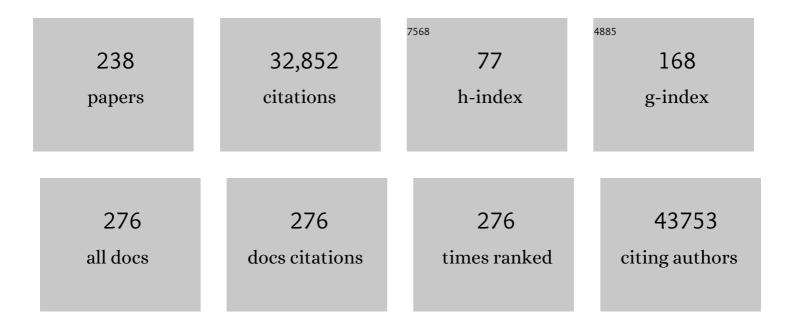


List of Publications by Year in descending order

Source: https://exaly.com/author-pdf/1442269/publications.pdf Version: 2024-02-01



Ηλο λλμ

#	Article	IF	CITATIONS
1	LIN28 coordinately promotes nucleolar/ribosomal functions and represses the 2C-like transcriptional program in pluripotent stem cells. Protein and Cell, 2022, 13, 490-512.	11.0	28
2	TRIM21 regulates pyroptotic cell death by promoting Gasdermin D oligomerization. Cell Death and Differentiation, 2022, 29, 439-450.	11.2	33
3	Advances toward structure-based drug discovery for inflammasome targets. Journal of Experimental Medicine, 2022, 219, .	8.5	2
4	SPARCLE, a p53-induced lncRNA, controls apoptosis after genotoxic stress by promoting PARP-1 cleavage. Molecular Cell, 2022, 82, 785-802.e10.	9.7	24
5	A comprehensive comparison of supervised and unsupervised methods for cell type identification in single-cell RNA-seq. Briefings in Bioinformatics, 2022, 23, .	6.5	22
6	Inflammasome Activation and Pyroptosis via a Lipid-regulated SIRT1-p53-ASC Axis in Macrophages From Male Mice and Humans. Endocrinology, 2022, 163, .	2.8	12
7	Electrostatic influence on IL-1 transport through the GSDMD pore. Proceedings of the National Academy of Sciences of the United States of America, 2022, 119, .	7.1	13
8	Targeting stem-loop 1 of the SARS-CoV-2 $5\hat{a}$ € ² UTR to suppress viral translation and Nsp1 evasion. Proceedings of the National Academy of Sciences of the United States of America, 2022, 119, .	7.1	56
9	Diabetes and Its Cardiovascular Complications: Comprehensive Network and Systematic Analyses. Frontiers in Cardiovascular Medicine, 2022, 9, 841928.	2.4	7
10	pH regulates potassium conductance and drives a constitutive proton current in human TMEM175. Science Advances, 2022, 8, eabm1568.	10.3	22
11	EDClust: an EM–MM hybrid method for cell clustering in multiple-subject single-cell RNA sequencing. Bioinformatics, 2022, 38, 2692-2699.	4.1	4
12	FcÎ ³ R-mediated SARS-CoV-2 infection of monocytes activates inflammation. Nature, 2022, 606, 576-584.	27.8	314
13	The Role of Endothelial-to-Mesenchymal Transition in Cardiovascular Disease. Cells, 2022, 11, 1834.	4.1	16
14	Structure of cytoplasmic ring of nuclear pore complex by integrative cryo-EM and AlphaFold. Science, 2022, 376, .	12.6	89
15	Epsins in vascular development, function and disease. Cellular and Molecular Life Sciences, 2021, 78, 833-842.	5.4	11
16	Multiple domain interfaces mediate SARM1 autoinhibition. Proceedings of the National Academy of Sciences of the United States of America, 2021, 118, .	7.1	54
17	Structure of a microtubule-bound axonemal dynein. Nature Communications, 2021, 12, 477.	12.8	54
18	Mechanism of filament formation in UPA-promoted CARD8 and NLRP1 inflammasomes. Nature Communications, 2021, 12, 189.	12.8	48

#	Article	IF	CITATIONS
19	Epsins 1 and 2 promote NEMO linear ubiquitination via LUBAC to drive breast cancer development. Journal of Clinical Investigation, 2021, 131, .	8.2	18
20	Accurate feature selection improves single-cell RNA-seq cell clustering. Briefings in Bioinformatics, 2021, 22, .	6.5	31
21	Cryo-EM structure of an activated GPCR–G protein complex in lipid nanodiscs. Nature Structural and Molecular Biology, 2021, 28, 258-267.	8.2	71
22	DPP9 sequesters the CÂterminus of NLRP1 to repress inflammasome activation. Nature, 2021, 592, 778-783.	27.8	114
23	Channelling inflammation: gasdermins in physiology and disease. Nature Reviews Drug Discovery, 2021, 20, 384-405.	46.4	323
24	Downregulation of <i>TOP2</i> modulates neurodegeneration caused by GGGGCC expanded repeats. Human Molecular Genetics, 2021, 30, 893-901.	2.9	4
25	Purification and cryoelectron microscopy structure determination of human V-ATPase. STAR Protocols, 2021, 2, 100350.	1.2	2
26	Detecting m6A methylation regions from Methylated RNA Immunoprecipitation Sequencing. Bioinformatics, 2021, 37, 2818-2824.	4.1	10
27	STING condensates on ER limit IFN response. Nature Cell Biology, 2021, 23, 299-300.	10.3	3
28	Gasdermin D pore structure reveals preferential release of mature interleukin-1. Nature, 2021, 593, 607-611.	27.8	298
29	NLRP3 Inflammasome Assembly in Neutrophils Is Supported by PAD4 and Promotes NETosis Under Sterile Conditions. Frontiers in Immunology, 2021, 12, 683803.	4.8	79
30	Structures and functions of the inflammasome engine. Journal of Allergy and Clinical Immunology, 2021, 147, 2021-2029.	2.9	35
31	Dipeptidyl peptidase 9 sets a threshold for CARD8 inflammasome formation by sequestering its active C-terminal fragment. Immunity, 2021, 54, 1392-1404.e10.	14.3	47
32	RIP1/RIP3/MLKL Mediates Myocardial Function Through Necroptosis in Experimental Autoimmune Myocarditis. Frontiers in Cardiovascular Medicine, 2021, 8, 696362.	2.4	7
33	Inflammasome activation at the crux of severe COVID-19. Nature Reviews Immunology, 2021, 21, 694-703.	22.7	210
34	Non-alcoholic Steatohepatitis Pathogenesis, Diagnosis, and Treatment. Frontiers in Cardiovascular Medicine, 2021, 8, 742382.	2.4	22
35	BTK operates a phospho-tyrosine switch to regulate NLRP3 inflammasome activity. Journal of Experimental Medicine, 2021, 218, .	8.5	33
36	Evaluation of some aspects in supervised cell type identification for single-cell RNA-seq: classifier, feature selection, and reference construction. Genome Biology, 2021, 22, 264.	8.8	21

#	Article	IF	CITATIONS
37	Could AlphaFold revolutionize chemical therapeutics?. Nature Structural and Molecular Biology, 2021, 28, 771-772.	8.2	30
38	Ragulator-Rag and ROS TORment gasdermin D pore formation. Trends in Immunology, 2021, 42, 948-950.	6.8	8
39	Nonmetastatic breast cancer patients subsequently developing second primary malignancy: A populationâ€based study. Cancer Medicine, 2021, 10, 8662-8672.	2.8	8
40	Phase separation drives RNA virus-induced activation of the NLRP6 inflammasome. Cell, 2021, 184, 5759-5774.e20.	28.9	97
41	Disulfiram use is associated with lower risk of COVID-19: A retrospective cohort study. PLoS ONE, 2021, 16, e0259061.	2.5	32
42	Expression Signatures of Long Noncoding RNAs in Left Ventricular Noncompaction. Frontiers in Cardiovascular Medicine, 2021, 8, 763858.	2.4	0
43	KDM1A Identified as a Potential Oncogenic Driver and Prognostic Biomarker via Multi-Omics Analysis. Canadian Journal of Infectious Diseases and Medical Microbiology, 2021, 2021, 1-18.	1.9	5
44	NLRP3 cages revealed by full-length mouse NLRP3 structure control pathway activation. Cell, 2021, 184, 6299-6312.e22.	28.9	120
45	A comprehensive review of computational prediction of genome-wide features. Briefings in Bioinformatics, 2020, 21, 120-134.	6.5	12
46	Combined immunodeficiency caused by a loss-of-function mutation in DNA polymerase delta 1. Journal of Allergy and Clinical Immunology, 2020, 145, 391-401.e8.	2.9	28
47	Age-related DNA hydroxymethylation is enriched for gene expression and immune system processes in human peripheral blood. Epigenetics, 2020, 15, 294-306.	2.7	8
48	Mechanism and Regulation of Gasdermin-Mediated Cell Death. Cold Spring Harbor Perspectives in Biology, 2020, 12, a036400.	5.5	100
49	METTL4 is an snRNA m6Am methyltransferase that regulates RNA splicing. Cell Research, 2020, 30, 544-547.	12.0	84
50	Ethnicity-specific and overlapping alterations of brain hydroxymethylome in Alzheimer's disease. Human Molecular Genetics, 2020, 29, 149-158.	2.9	11
51	Discovery of a Selective, Covalent IRAK1 Inhibitor with Antiproliferative Activity in MYD88 Mutated B-Cell Lymphoma. ACS Medicinal Chemistry Letters, 2020, 11, 2238-2243.	2.8	11
52	Structures of a Complete Human V-ATPase Reveal Mechanisms of Its Assembly. Molecular Cell, 2020, 80, 501-511.e3.	9.7	88
53	Epsin-mediated degradation of IP3R1 fuels atherosclerosis. Nature Communications, 2020, 11, 3984.	12.8	24
54	HDAC6 mediates an aggresome-like mechanism for NLRP3 and pyrin inflammasome activation. Science, 2020, 369, .	12.6	218

#	Article	IF	CITATIONS
55	FDA-approved disulfiram inhibits pyroptosis by blocking gasdermin D pore formation. Nature Immunology, 2020, 21, 736-745.	14.5	555
56	Gain-of-function mutations in CARD11 promote enhanced aggregation and idiosyncratic signalosome assembly. Cellular Immunology, 2020, 353, 104129.	3.0	7
57	Homogeneous Oligomers of Pro-apoptotic BAX Reveal Structural Determinants of Mitochondrial Membrane Permeabilization. Molecular Cell, 2020, 79, 68-83.e7.	9.7	32
58	A nanobody targeting the LIN28:let-7 interaction fragment of TUT4 blocks uridylation of let-7. Proceedings of the National Academy of Sciences of the United States of America, 2020, 117, 4653-4663.	7.1	15
59	Gasdermin E suppresses tumour growth by activating anti-tumour immunity. Nature, 2020, 579, 415-420.	27.8	900
60	CG14906 (mettl4) mediates m6A methylation of U2 snRNA in Drosophila. Cell Discovery, 2020, 6, 44.	6.7	35
61	TRPM2, linking oxidative stress and Ca2+ permeation to NLRP3 inflammasome activation. Current Opinion in Immunology, 2020, 62, 131-135.	5.5	54
62	An Acetylation Switch of the NLRP3 Inflammasome Regulates Aging-Associated Chronic Inflammation and Insulin Resistance. Cell Metabolism, 2020, 31, 580-591.e5.	16.2	213
63	Higher-order assemblies in innate immune and inflammatory signaling: A general principle in cell biology. Current Opinion in Cell Biology, 2020, 63, 194-203.	5.4	24
64	Modulation of virus-induced NF-κB signaling by NEMO coiled coil mimics. Nature Communications, 2020, 11, 1786.	12.8	30
65	BCL10 Gain-of-Function Mutations Aberrantly Induce Canonical and Non-Canonical NF-Kb Activation and Resistance to Ibrutinib in ABC-DLBCL. Blood, 2020, 136, 2-3.	1.4	4
66	CDKL3 promotes osteosarcoma progression by activating Akt/PKB. Life Science Alliance, 2020, 3, e202000648.	2.8	7
67	Inhibition of histone lysine-specific demethylase 1 elicits breast tumor immunity and enhances antitumor efficacy of immune checkpoint blockade. Oncogene, 2019, 38, 390-405.	5.9	149
68	Michael G. Rossmann (1930–2019). Nature Structural and Molecular Biology, 2019, 26, 660-662.	8.2	3
69	Keeping the Death Protein in Check. Immunity, 2019, 51, 1-2.	14.3	22
70	Gasdermin D activity in inflammation and host defense. Science Immunology, 2019, 4, .	11.9	119
71	TOAST: improving reference-free cell composition estimation by cross-cell type differential analysis. Genome Biology, 2019, 20, 190.	8.8	42
72	Conformational flexibility and inhibitor binding to unphosphorylated interleukin-1 receptor–associated kinase 4 (IRAK4). Journal of Biological Chemistry, 2019, 294, 4511-4519.	3.4	14

#	Article	IF	CITATIONS
73	SERPINB1-mediated checkpoint of inflammatory caspase activation. Nature Immunology, 2019, 20, 276-287.	14.5	87
74	Mimicry by a viral <scp>RHIM</scp> . EMBO Reports, 2019, 20, .	4.5	7
75	Molecular mechanism for NLRP6 inflammasome assembly and activation. Proceedings of the National Academy of Sciences of the United States of America, 2019, 116, 2052-2057.	7.1	86
76	Mechanism of TRPM 2 channel gating revealed by cryo―EM. FEBS Journal, 2019, 286, 3333-3339.	4.7	12
77	Monitoring gasdermin pore formation in vitro. Methods in Enzymology, 2019, 625, 95-107.	1.0	20
78	Structural mechanism for NEK7-licensed activation of NLRP3 inflammasome. Nature, 2019, 570, 338-343.	27.8	467
79	Structural and mechanistic elucidation of inflammasome signaling by cryo-EM. Current Opinion in Structural Biology, 2019, 58, 18-25.	5.7	23
80	Quinoline and thiazolopyridine allosteric inhibitors of MALT1. Bioorganic and Medicinal Chemistry Letters, 2019, 29, 1694-1698.	2.2	14
81	Reactivation of PTEN tumor suppressor for cancer treatment through inhibition of a MYC-WWP1 inhibitiory pathway. Science, 2019, 364, .	12.6	194
82	Dissecting differential signals in high-throughput data from complex tissues. Bioinformatics, 2019, 35, 3898-3905.	4.1	35
83	Peptide-based covalent inhibitors of MALT1 paracaspase. Bioorganic and Medicinal Chemistry Letters, 2019, 29, 1336-1339.	2.2	15
84	Higher-Order Clustering of the Transmembrane Anchor of DR5 Drives Signaling. Cell, 2019, 176, 1477-1489.e14.	28.9	104
85	Michael G. Rossmann (1930–2019), pioneer in macromolecular and virus crystallography: scientist, mentor and friend. Acta Crystallographica Section D: Structural Biology, 2019, 75, 523-527.	2.3	0
86	Differential methylation analysis for bisulfite sequencing using DSS. Quantitative Biology, 2019, 7, 327-334.	0.5	21
87	Myeloid-Specific Deletion of Epsins 1 and 2 Reduces Atherosclerosis by Preventing LRP-1 Downregulation. Circulation Research, 2019, 124, e6-e19.	4.5	41
88	Crystal structure of the WD40 domain dimer of LRRK2. Proceedings of the National Academy of Sciences of the United States of America, 2019, 116, 1579-1584.	7.1	60
89	Disease prediction by cell-free DNA methylation. Briefings in Bioinformatics, 2019, 20, 585-597.	6.5	35
90	Structural Basis for NLRP6 Inflammasome Assembly and Activation. FASEB Journal, 2019, 33, 779.38.	0.5	0

#	Article	IF	CITATIONS
91	Insights into gasdermin pore formation from the structure of a preâ€pore. FASEB Journal, 2019, 33, 779.49.	0.5	1
92	Enhanced Lymphangiogenesis and Lymphatic Function Protects Dietâ€induced Obesity and Insulin Resistance. FASEB Journal, 2019, 33, 662.25.	0.5	1
93	Higherâ€Order Clustering of the Transmembrane Anchor of DR5 Drives Signaling. FASEB Journal, 2019, 33, 792.3.	0.5	0
94	Structures and gating mechanism of human TRPM2. FASEB Journal, 2019, 33, .	0.5	0
95	The Structure of the Necrosome RIPK1-RIPK3 Core, a Human Hetero-Amyloid Signaling Complex. Cell, 2018, 173, 1244-1253.e10.	28.9	216
96	Two-phase differential expression analysis for single cell RNA-seq. Bioinformatics, 2018, 34, 3340-3348.	4.1	34
97	Cryo-EM structure of the gasdermin A3 membrane pore. Nature, 2018, 557, 62-67.	27.8	301
98	HDAC5–LSD1 axis regulates antineoplastic effect of natural HDAC inhibitor sulforaphane in human breast cancer cells. International Journal of Cancer, 2018, 143, 1388-1401.	5.1	54
99	Mind Bomb Regulates Cell Death during TNF Signaling by Suppressing RIPK1's Cytotoxic Potential. Cell Reports, 2018, 23, 470-484.	6.4	42
100	Ubiquitin-Mediated Regulation of RIPK1 Kinase Activity Independent of IKK and MK2. Molecular Cell, 2018, 69, 566-580.e5.	9.7	102
101	Inflammation NODs to Antagonists of RIP2-XIAP Interaction. Molecular Cell, 2018, 69, 535-536.	9.7	2
102	Bad germs are trapped. Cell Research, 2018, 28, 141-142.	12.0	4
103	Assembly mechanism of the CARMA1–BCL10–MALT1–TRAF6 signalosome. Proceedings of the National Academy of Sciences of the United States of America, 2018, 115, 1499-1504.	7.1	87
104	Epitranscriptomic m6A Regulation of Axon Regeneration in the Adult Mammalian Nervous System. Neuron, 2018, 97, 313-325.e6.	8.1	292
105	Mechanism of ubiquitin transfer promoted by TRAF6. Proceedings of the National Academy of Sciences of the United States of America, 2018, 115, 1783-1788.	7.1	34
106	The nuclear matrix protein HNRNPU maintains 3D genome architecture globally in mouse hepatocytes. Genome Research, 2018, 28, 192-202.	5.5	91
107	InfiniumPurify: An R package for estimating and accounting for tumor purity in cancer methylation research. Genes and Diseases, 2018, 5, 43-45.	3.4	48
108	A High Throughput Whole Blood Assay for Analysis of Multiple Antigen-Specific T Cell Responses in Human <i>Mycobacterium tuberculosis</i> Infection. Journal of Immunology, 2018, 200, 3008-3019.	0.8	11

#	Article	IF	CITATIONS
109	Fibrinogenâ€like proteinâ€2 causes deterioration in cardiac function in experimental autoimmune myocarditis rats through regulation of programmed deathâ€1 and inflammatory cytokines. Immunology, 2018, 153, 246-252.	4.4	13
110	The Pore-Forming Protein Gasdermin D Regulates Interleukin-1 Secretion from Living Macrophages. Immunity, 2018, 48, 35-44.e6.	14.3	789
111	FGL2 knockdown improves heart function through regulation of TLR9 signaling in the experimental autoimmune myocarditis rats. Immunologic Research, 2018, 66, 52-58.	2.9	7
112	Structural gymnastics of RAG-mediated DNA cleavage in V(D)J recombination. Current Opinion in Structural Biology, 2018, 53, 178-186.	5.7	20
113	Structures and gating mechanism of human TRPM2. Science, 2018, 362, .	12.6	129
114	Ten-Eleven Translocation Proteins Modulate the Response to Environmental Stress in Mice. Cell Reports, 2018, 25, 3194-3203.e4.	6.4	46
115	Cryo-EM structures of ASC and NLRC4 CARD filaments reveal a unified mechanism of nucleation and activation of caspase-1. Proceedings of the National Academy of Sciences of the United States of America, 2018, 115, 10845-10852.	7.1	103
116	Ectopic lipid accumulation: potential role in tubular injury and inflammation in diabetic kidney disease. Clinical Science, 2018, 132, 2407-2422.	4.3	53
117	Pathogen blockade of TAK1 triggers caspase-8–dependent cleavage of gasdermin D and cell death. Science, 2018, 362, 1064-1069.	12.6	639
118	5-Hydroxymethylcytosine alterations in the human postmortem brains of autism spectrum disorder. Human Molecular Genetics, 2018, 27, 2955-2964.	2.9	28
119	DNA melting initiates the RAG catalytic pathway. Nature Structural and Molecular Biology, 2018, 25, 732-742.	8.2	40
120	Active N6-Methyladenine Demethylation by DMAD Regulates Gene Expression by Coordinating with Polycomb Protein in Neurons. Molecular Cell, 2018, 71, 848-857.e6.	9.7	71
121	Gene expression profiles of rat MMECs with different glucose levels and <i>fgl2</i> gene silencing. Diabetes/Metabolism Research and Reviews, 2018, 34, e3058.	4.0	0
122	Fragile X mental retardation protein modulates the stability of its m6A-marked messenger RNA targets. Human Molecular Genetics, 2018, 27, 3936-3950.	2.9	129
123	Epsin deficiency promotes lymphangiogenesis through regulation of VEGFR3 degradation in diabetes. Journal of Clinical Investigation, 2018, 128, 4025-4043.	8.2	52
124	Specific covalent inhibition of MALT1 paracaspase suppresses B cell lymphoma growth. Journal of Clinical Investigation, 2018, 128, 4397-4412.	8.2	51
125	INAVA-ARNO complexes bridge mucosal barrier function with inflammatory signaling. ELife, 2018, 7, .	6.0	17
126	Ruxolitinib reverses dysregulated T helper cell responses and controls autoimmunity caused by a novel signal transducer and activator of transcription 1 (STAT1) gain-of-function mutation. Journal of Allergy and Clinical Immunology, 2017, 139, 1629-1640.e2.	2.9	147

#	Article	IF	CITATIONS
127	A genomeâ€wide profiling of brain DNA hydroxymethylation in Alzheimer's disease. Alzheimer's and Dementia, 2017, 13, 674-688.	0.8	83
128	Epigenomic reprogramming during pancreatic cancer progression links anabolic glucose metabolism to distant metastasis. Nature Genetics, 2017, 49, 367-376.	21.4	365
129	Mapping the Broad Structural and Mechanical Properties of Amyloid Fibrils. Biophysical Journal, 2017, 112, 584-594.	0.5	40
130	PLEMT: A Novel Pseudolikelihood-Based EM Test for Homogeneity in Generalized Exponential Tilt Mixture Models. Journal of the American Statistical Association, 2017, 112, 1393-1404.	3.1	7
131	Instant Hydrogelation Inspired by Inflammasomes. Angewandte Chemie - International Edition, 2017, 56, 7579-7583.	13.8	22
132	Instant Hydrogelation Inspired by Inflammasomes. Angewandte Chemie, 2017, 129, 7687-7691.	2.0	7
133	Sirolimus for the treatment of progressive kaposiform hemangioendothelioma: A multicenter retrospective study. International Journal of Cancer, 2017, 141, 848-855.	5.1	103
134	Accounting for tumor purity improves cancer subtype classification from DNA methylation data. Bioinformatics, 2017, 33, 2651-2657.	4.1	32
135	Understanding CARD Tricks in Apoptosomes. Structure, 2017, 25, 575-577.	3.3	8
136	Disulfide Bond Formation and N-Glycosylation Modulate Protein-Protein Interactions in GPI-Transamidase (GPIT). Scientific Reports, 2017, 7, 45912.	3.3	10
137	Differential gene network analysis from single cell RNA-seq. Journal of Genetics and Genomics, 2017, 44, 331-334.	3.9	7
138	Evidence for M1-Linked Polyubiquitin-Mediated Conformational Change in NEMO. Journal of Molecular Biology, 2017, 429, 3793-3800.	4.2	27
139	Peptidoglycan-Sensing Receptors Trigger the Formation of Functional Amyloids of the Adaptor Protein Imd to Initiate Drosophila NF-I°B Signaling. Immunity, 2017, 47, 635-647.e6.	14.3	63
140	DNA N6-methyladenine is dynamically regulated in the mouse brain following environmental stress. Nature Communications, 2017, 8, 1122.	12.8	182
141	Integrating Next-Generation Genomic Sequencing and Mass Spectrometry To Estimate Allele-Specific Protein Abundance in Human Brain. Journal of Proteome Research, 2017, 16, 3336-3347.	3.7	48
142	AID Recognizes Structured DNA for Class Switch Recombination. Molecular Cell, 2017, 67, 361-373.e4.	9.7	136
143	Zika virus directly infects peripheral neurons and induces cell death. Nature Neuroscience, 2017, 20, 1209-1212.	14.8	85
144	CIDE domains form functionally important higher-order assemblies for DNA fragmentation. Proceedings of the National Academy of Sciences of the United States of America, 2017, 114, 7361-7366.	7.1	23

#	Article	IF	CITATIONS
145	Cryo-EM structure of the DNA-PK holoenzyme. Proceedings of the National Academy of Sciences of the United States of America, 2017, 114, 7367-7372.	7.1	74
146	Estimating and accounting for tumor purity in the analysis of DNA methylation data from cancer studies. Genome Biology, 2017, 18, 17.	8.8	112
147	Ten-eleven translocation 2 interacts with forkhead box O3 and regulates adult neurogenesis. Nature Communications, 2017, 8, 15903.	12.8	82
148	Role of endoplasmic reticulum stress signalling in diabetic endothelial dysfunction and atherosclerosis. Diabetes and Vascular Disease Research, 2017, 14, 14-23.	2.0	83
149	Endothelial epsins as regulators and potential therapeutic targets of tumor angiogenesis. Cellular and Molecular Life Sciences, 2017, 74, 393-398.	5.4	12
150	ROC Curve Analysis in the Presence of Imperfect Reference Standards. Statistics in Biosciences, 2017, 9, 91-104.	1.2	13
151	Eating the Dead to Keep Atherosclerosis at Bay. Frontiers in Cardiovascular Medicine, 2017, 4, 2.	2.4	54
152	Crystal structure of human IRAK1. Proceedings of the National Academy of Sciences of the United States of America, 2017, 114, 13507-13512.	7.1	59
153	Functional characterization of lysine-specific demethylase 2 (LSD2/KDM1B) in breast cancer progression. Oncotarget, 2017, 8, 81737-81753.	1.8	34
154	Mimetic peptide of ubiquitin-interacting motif of epsin as a cancer therapeutic-perspective in brain tumor therapy through regulating VEGFR2 signaling. Vessel Plus, 2017, 1, 3-11.	0.4	8
155	Inflammasome-activated gasdermin D causes pyroptosis by forming membrane pores. Nature, 2016, 535, 153-158.	27.8	2,143
156	Characterization of T and B cell repertoire diversity in patients with RAG deficiency. Science Immunology, 2016, 1, .	11.9	88
157	Molecular basis of caspase-1 polymerization and its inhibition by a new capping mechanism. Nature Structural and Molecular Biology, 2016, 23, 416-425.	8.2	135
158	The Structure and Dynamics of Higher-Order Assemblies: Amyloids, Signalosomes, and Granules. Cell, 2016, 165, 1055-1066.	28.9	311
159	Tumor purity and differential methylation in cancer epigenomics. Briefings in Functional Genomics, 2016, 15, elw016.	2.7	13
160	An endogenous caspase-11 ligand elicits interleukin-1 release from living dendritic cells. Science, 2016, 352, 1232-1236.	12.6	419
161	Brain-Region-Specific Organoids Using Mini-bioreactors for Modeling ZIKV Exposure. Cell, 2016, 165, 1238-1254.	28.9	1,680
162	A single domain antibody fragment that recognizes the adaptor ASC defines the role of ASC domains in inflammasome assembly. Journal of Experimental Medicine, 2016, 213, 771-790.	8.5	145

#	Article	lF	CITATIONS
163	Base-resolution profiling of active DNA demethylation using MAB-seq and caMAB-seq. Nature Protocols, 2016, 11, 1081-1100.	12.0	30
164	Molecular signatures associated with ZIKV exposure in human cortical neural progenitors. Nucleic Acids Research, 2016, 44, 8610-8620.	14.5	155
165	Cryo-EM Structure of Caspase-8 Tandem DED Filament Reveals Assembly and Regulation Mechanisms of the Death-Inducing Signaling Complex. Molecular Cell, 2016, 64, 236-250.	9.7	128
166	NanoStringDiff: a novel statistical method for differential expression analysis based on NanoString nCounter data. Nucleic Acids Research, 2016, 44, gkw677.	14.5	100
167	Inhibition of ileal bile acid uptake protects against nonalcoholic fatty liver disease in high-fat diet–fed mice. Science Translational Medicine, 2016, 8, 357ra122.	12.4	160
168	Dedicator of cytokinesis 8 regulates signal transducer and activator of transcription 3 activation and promotes TH17Âcell differentiation. Journal of Allergy and Clinical Immunology, 2016, 138, 1384-1394.e2.	2.9	70
169	Lin28A Binds Active Promoters and Recruits Tet1 to Regulate Gene Expression. Molecular Cell, 2016, 61, 153-160.	9.7	74
170	Statistical Challenges in Analyzing Methylation and Long-Range Chromosomal Interaction Data. Statistics in Biosciences, 2016, 8, 284-309.	1.2	9
171	Experimental Design and Power Calculation for RNA-seq Experiments. Methods in Molecular Biology, 2016, 1418, 379-390.	0.9	13
172	Measuring the spatial correlations of protein binding sites. Bioinformatics, 2016, 32, 1766-1772.	4.1	2
173	Selective Targeting of a Novel Epsin–VEGFR2 Interaction Promotes VEGF-Mediated Angiogenesis. Circulation Research, 2016, 118, 957-969.	4.5	35
174	Structural Basis and Functional Role of Intramembrane Trimerization of the Fas/CD95 Death Receptor. Molecular Cell, 2016, 61, 602-613.	9.7	135
175	Differential methylation analysis for BS-seq data under general experimental design. Bioinformatics, 2016, 32, 1446-1453.	4.1	336
176	Supramolecular organizing centers (SMOCs) as signaling machines in innate immune activation. Science China Life Sciences, 2015, 58, 1067-1072.	4.9	14
177	Plasticity in PYD assembly revealed by cryo-EM structure of the PYD filament of AIM2. Cell Discovery, 2015, 1, .	6.7	83
178	Local false discovery rate estimation using feature reliability in LC/MS metabolomics data. Scientific Reports, 2015, 5, 17221.	3.3	24
179	MacroH2A1 associates with nuclear lamina and maintains chromatin architecture in mouse liver cells. Scientific Reports, 2015, 5, 17186.	3.3	44
180	Computer Simulation, Bioinformatics, and Statistical Analysis of Cancer Data and Processes. Cancer Informatics, 2015, 14s2, CIN.S32525.	1.9	0

#	Article	IF	CITATIONS
181	Base-resolution methylation patterns accurately predict transcription factor bindings in vivo. Nucleic Acids Research, 2015, 43, 2757-2766.	14.5	46
182	The Inflammasome Adaptor ASC Induces Procaspase-8 Death Effector Domain Filaments. Journal of Biological Chemistry, 2015, 290, 29217-29230.	3.4	69
183	A Specific LSD1/KDM1A Isoform Regulates Neuronal Differentiation through H3K9 Demethylation. Molecular Cell, 2015, 57, 957-970.	9.7	221
184	Long-Lived Plasma Cells Are Contained within the CD19â^'CD38hiCD138+ Subset in Human Bone Marrow. Immunity, 2015, 43, 132-145.	14.3	415
185	The hierarchical structural architecture of inflammasomes, supramolecular inflammatory machines. Current Opinion in Structural Biology, 2015, 31, 75-83.	5.7	58
186	Plasmodium knowlesi gene expression differs in ex vivo compared to in vitro blood-stage cultures. Malaria Journal, 2015, 14, 110.	2.3	31
187	A novel statistical method for quantitative comparison of multiple ChIP-seq datasets. Bioinformatics, 2015, 31, 1889-1896.	4.1	48
188	The ubiquitin-modifying enzyme A20 restricts ubiquitination of the kinase RIPK3 and protects cells from necroptosis. Nature Immunology, 2015, 16, 618-627.	14.5	224
189	Active Pin1 is a key target of all-trans retinoic acid in acute promyelocytic leukemia and breast cancer. Nature Medicine, 2015, 21, 457-466.	30.7	220
190	Molecular Mechanism of V(D)J Recombination from Synaptic RAG1-RAG2 Complex Structures. Cell, 2015, 163, 1138-1152.	28.9	154
191	Predicting tumor purity from methylation microarray data. Bioinformatics, 2015, 31, 3401-3405.	4.1	50
192	Cryo-EM structure of the activated NAIP2-NLRC4 inflammasome reveals nucleated polymerization. Science, 2015, 350, 404-409.	12.6	347
193	Detection of differentially methylated regions from whole-genome bisulfite sequencing data without replicates. Nucleic Acids Research, 2015, 43, gkv715.	14.5	203
194	PROPER: comprehensive power evaluation for differential expression using RNA-seq. Bioinformatics, 2015, 31, 233-241.	4.1	80
195	PolyaPeak: Detecting Transcription Factor Binding Sites from ChIP-seq Using Peak Shape Information. PLoS ONE, 2014, 9, e89694.	2.5	13
196	Incorporating feature reliability in false discovery rateestimation improves statistical power to detect differentially expressed features. , 2014, , .		0
197	A Bayesian hierarchical model to detect differentially methylated loci from single nucleotide resolution sequencing data. Nucleic Acids Research, 2014, 42, e69-e69.	14.5	405
198	Hydrolysis of 2′3′-cGAMP by ENPP1 and design of nonhydrolyzable analogs. Nature Chemical Biology, 2014, 10, 1043-1048.	8.0	348

#	Article	IF	CITATIONS
199	IRAK4 Dimerization and trans -Autophosphorylation Are Induced by Myddosome Assembly. Molecular Cell, 2014, 55, 891-903.	9.7	108
200	Genome-wide alteration of 5-hydroxymethylcytosine in a mouse model of fragile X-associated tremor/ataxia syndrome. Human Molecular Genetics, 2014, 23, 1095-1107.	2.9	52
201	Modeling Parkinson's disease in monkeys for translational studies, a critical analysis. Experimental Neurology, 2014, 256, 133-143.	4.1	62
202	Promiscuity Is Not Always Bad. Molecular Cell, 2014, 54, 208-209.	9.7	3
203	Crystal Structure of the F27G AIM2 PYD Mutant and Similarities of Its Self-Association to DED/DED Interactions. Journal of Molecular Biology, 2014, 426, 1420-1427.	4.2	51
204	Unified Polymerization Mechanism for the Assembly of ASC-Dependent Inflammasomes. Cell, 2014, 156, 1193-1206.	28.9	1,035
205	Reversing DNA Methylation: Mechanisms, Genomics, and Biological Functions. Cell, 2014, 156, 45-68.	28.9	914
206	Single-base resolution analysis of active DNA demethylation using methylase-assisted bisulfite sequencing. Nature Biotechnology, 2014, 32, 1231-1240.	17.5	139
207	Deletion of Atbf1/Zfhx3 In Mouse Prostate Causes Neoplastic Lesions, Likely by Attenuation of Membrane and Secretory Proteins and Multiple Signaling Pathways. Neoplasia, 2014, 16, 377-389.	5.3	31
208	The CBM signalosome: Potential therapeutic target for aggressive lymphoma?. Cytokine and Growth Factor Reviews, 2014, 25, 175-183.	7.2	14
209	HMMR Maintains the Stemness and Tumorigenicity of Glioblastoma Stem-like Cells. Cancer Research, 2014, 74, 3168-3179.	0.9	101
210	U1 small nuclear ribonucleoprotein complex and RNA splicing alterations in Alzheimer's disease. Proceedings of the National Academy of Sciences of the United States of America, 2013, 110, 16562-16567.	7.1	268
211	Cell-Cycle Control of Developmentally Regulated Transcription Factors Accounts for Heterogeneity in Human Pluripotent Cells. Stem Cell Reports, 2013, 1, 532-544.	4.8	129
212	Kdm2b maintains murine embryonic stem cell status by recruiting PRC1 complex to CpG islands of developmental genes. Nature Cell Biology, 2013, 15, 373-384.	10.3	292
213	A new shrinkage estimator for dispersion improves differential expression detection in RNA-seq data. Biostatistics, 2013, 14, 232-243.	1.5	210
214	Higher-Order Assemblies in a New Paradigm of Signal Transduction. Cell, 2013, 153, 287-292.	28.9	291
215	Genome-wide Profiling of 5-Formylcytosine Reveals Its Roles in Epigenetic Priming. Cell, 2013, 153, 678-691.	28.9	502
216	Genome-wide Analysis Reveals TET- and TDG-Dependent 5-Methylcytosine Oxidation Dynamics. Cell, 2013, 153, 692-706.	28.9	440

#	Article	IF	CITATIONS
217	Subtelomeric hotspots of aberrant 5-hydroxymethylcytosine-mediated epigenetic modifications during reprogramming to pluripotency. Nature Cell Biology, 2013, 15, 700-711.	10.3	87
218	Exploring the Cooccurrence Patterns of Multiple Sets of Genomic Intervals. BioMed Research International, 2013, 2013, 1-7.	1.9	2
219	Fragile X premutation RNA is sufficient to cause primary ovarian insufficiency in mice. Human Molecular Genetics, 2012, 21, 5039-5047.	2.9	78
220	Genome-wide DNA hydroxymethylation changes are associated with neurodevelopmental genes in the developing human cerebellum. Human Molecular Genetics, 2012, 21, 5500-5510.	2.9	157
221	Euchromatin islands in large heterochromatin domains are enriched for CTCF binding and differentially DNA-methylated regions. BMC Genomics, 2012, 13, 566.	2.8	40
222	Statistics for Next Generation Sequencing – Meeting Report. Frontiers in Genetics, 2012, 3, 128.	2.3	0
223	JAMIE: A Software Tool for Jointly Analyzing Multiple ChIP-chip Experiments. Methods in Molecular Biology, 2012, 802, 363-375.	0.9	1
224	Increased methylation variation in epigenetic domains across cancer types. Nature Genetics, 2011, 43, 768-775.	21.4	968
225	5-hmC–mediated epigenetic dynamics during postnatal neurodevelopment and aging. Nature Neuroscience, 2011, 14, 1607-1616.	14.8	746
226	Genome-scale epigenetic reprogramming during epithelial-to-mesenchymal transition. Nature Structural and Molecular Biology, 2011, 18, 867-874.	8.2	340
227	Reply to "Reassessing the abundance of H3K9me2 chromatin domains in embryonic stem cells― Nature Genetics, 2010, 42, 5-6.	21.4	32
228	Intensity normalization improves color calling in SOLiD sequencing. Nature Methods, 2010, 7, 336-337.	19.0	31
229	JAMIE: joint analysis of multiple ChIP-chip experiments. Bioinformatics, 2010, 26, 1864-1870.	4.1	12
230	Redefining CpG islands using hidden Markov models. Biostatistics, 2010, 11, 499-514.	1.5	151
231	A species-generalized probabilistic model-based definition of CpG islands. Mammalian Genome, 2009, 20, 674-80.	2.2	52
232	Large histone H3 lysine 9 dimethylated chromatin blocks distinguish differentiated from embryonic stem cells. Nature Genetics, 2009, 41, 246-250.	21.4	540
233	Comprehensive high-throughput arrays for relative methylation (CHARM). Genome Research, 2008, 18, 780-790.	5.5	379
234	Overlapping euchromatin/heterochromatin- associated marks are enriched in imprinted gene regions and predict allele-specific modification. Genome Research, 2008, 18, 1806-1813	5.5	29

#	Article	IF	Citations
235	R/qtlbim: QTL with Bayesian Interval Mapping in experimental crosses. Bioinformatics, 2007, 23, 641-643.	4.1	115
236	R/qtl: QTL mapping in experimental crosses. Bioinformatics, 2003, 19, 889-890.	4.1	3,197
237	FDA-approved disulfiram inhibits pyroptosis by blocking gasdermin D pore formation. , 0, .		1
238	<i>BCL10</i> Mutations Define Distinct Dependencies Guiding Precision Therapy for DLBCL. Cancer Discovery, 0, , OF1-OF20.	9.4	2